Dose-dependent changes in cardiac function, strain and remodelling in a preclinical model of heart base irradiation

Radiotherapy and Oncology 193 (2024) 110113

Contents lists available at ScienceDirect

Radiotherapy and Oncology

journal homepage: www.thegreenjournal.com

Original Article

Dose-dependent changes in cardiac function, strain and remodelling in a preclinical model of heart base irradiation

Mihaela Ghita-Pettigrew [a,*], Kevin S. Edgar [b], Refik Kuburas [a], Kathryn H. Brown [a], Gerard M. Walls [a,c], Cecilia Facchi [d], David J. Grieve [b], Chris J. Watson [b], Alan McWilliam [e], Marcel van Herk [e], Kaye J. Williams [d], Karl T. Butterworth [a]

[a] Patrick G. Johnston Centre for Cancer Research, Queen's University Belfast, Belfast, United Kingdom
[b] Wellcome-Wolfson Institute for Experimental Medicine, Queen's University Belfast, Belfast, United Kingdom
[c] Cancer Centre Belfast City Hospital, Belfast Health & Social Care Trust, Lisburn Road, Belfast, Northern Ireland
[d] Division of Pharmacy and Optometry, University of Manchester, Manchester, United Kingdom
[e] Department of Radiotherapy Related Research, University of Manchester, Manchester, United Kingdom

ARTICLE INFO

Keywords:
Cardiac toxicity
Preclinical radiotherapy
Cardiac strain
Heart base
Mouse model
Small animal radiotherapy

ABSTRACT

Background and purpose: Radiation induced cardiotoxicity (RICT) is as an important sequela of radiotherapy to the thorax for patients. In this study, we aim to investigate the dose and fractionation response of RICT. We propose global longitudinal strain (GLS) as an early indicator of RICT and investigate myocardial deformation following irradiation.

Methods: RICT was investigated in female C57BL/6J mice in which the base of the heart was irradiated under image-guidance using a small animal radiation research platform (SARRP). Mice were randomly assigned to a treatment group: single-fraction dose of 16 Gy or 20 Gy, 3 consecutive fractions of 8.66 Gy, or sham irradiation; biological effective doses (BED) used were 101.3 Gy, 153.3 Gy and 101.3 Gy respectively. Longitudinal transthoracic echocardiography (TTE) was performed from baseline up to 50 weeks post-irradiation to detect structural and functional effects.

Results: Irradiation of the heart base leads to BED-dependent changes in systolic and diastolic function 50 weeks post-irradiation. GLS showed significant decreases in a BED-dependent manner for all irradiated animals, as early as 10 weeks after irradiation. Early changes in GLS indicate late changes in cardiac function. BED-independent increases were observed in the left ventricle (LV) mass and volume and myocardial fibrosis.

Conclusions: Functional features of RICT displayed a BED dependence in this study. GLS showed an early change at 10 weeks post-irradiation. Cardiac remodelling was observed as increases in mass and volume of the LV, further supporting our hypothesis that dose to the base of the heart drives the global heart toxicity.

Introduction

Advances in conformal radiotherapy (RT) techniques and image-guidance have significantly reduced organs at risk (OAR) exposure, which has been associated with improved safety profiles [1]. However, opportunities remain to further optimise treatments based on the preferential avoidance of discrete radiosensitive subregions of OARs that have functional significance [2].

This has been demonstrated in the context of radiation cardiotoxicity, a late occurring toxicity for a high proportion of patients receiving treatment for thoracic malignancies, in terms of symptomatic cardiac events [3]. The heart has been recently identified to have a complex regional radiosensitivity [4]. Clinical studies have reported on specific regions of the heart where a higher dose bath was associated with decreased survival [5,6].

Murine models of RICT have been used to investigate the RT response of the heart, predicated on their genetic and physiological similarities with humans, as well as their accelerated lifespan, low maintenance and suitability for generating transgenic strains [7,8]. Previously, clinical findings have been reverse-translated to develop a novel preclinical model of sub-volume irradiation in the heart, validating the heart base as a radiosensitive sub-volume [9]. At molecular

* Corresponding author.
E-mail address: m.pettigrew@qub.ac.uk (M. Ghita-Pettigrew).

https://doi.org/10.1016/j.radonc.2024.110113
Received 15 August 2023; Received in revised form 24 January 2024; Accepted 25 January 2024
Available online 1 February 2024

level, spatial transcriptomics was used to gain detailed insight into the underlying basis of regional radiation response in the heart. These responses include the upregulation of immune-related processes and the downregulation of calcium transmembrane transporter activity, regulation of heart contraction and cytokine-mediated pathways [10].

The early detection and monitoring of cardiac function are crucial for patients who have undergone radiation therapy to help identify any potential complications and initiate further appropriate interventions. Global longitudinal strain (GLS) is an emerging echocardiography biomarker in the clinic that can be used to detect early left ventricular dysfunction. This approach uses a speckle tracking technique which can be used for reliable assessment of cardiac function and has been shown to detect RICT earlier than conventional parameters [11]. Clinical studies have analysed the GLS and segmental strain after breast radiotherapy and found variations in both at 6 months after irradiation [12]. Preclinical strain analysis is becoming increasingly feasible, as reported in recent murine models of cardiotoxicity [13,14].

In this study, we aimed to assess the functional consequences of cardiac base irradiation to establish the dose response relationship to specific biologically effective doses (BEDs). In addition, we aimed to demonstrate the predictive potential of global and segmental longitudinal strain GLS as early biomarkers for late occurring RICT.

Materials and methods

Animals and maintenance

RICT was investigated in female C57BL/6J mice 12–15 weeks old obtained from Charles River Laboratories (Oxford, UK). All mice were housed and handled as previously described [9]. Based on previous studies, the variation in myocardial performance index (MPI) within each group was expected to be approximately 15 %. Animal numbers were chosen to give power to detect differences in MPI of 25 % with a power of 80 % for a 2-sided equality test with a significance threshold of 0.05 which required at least six mice per group. Mice weights were monitored throughout the experiment showing minor fluctuations but

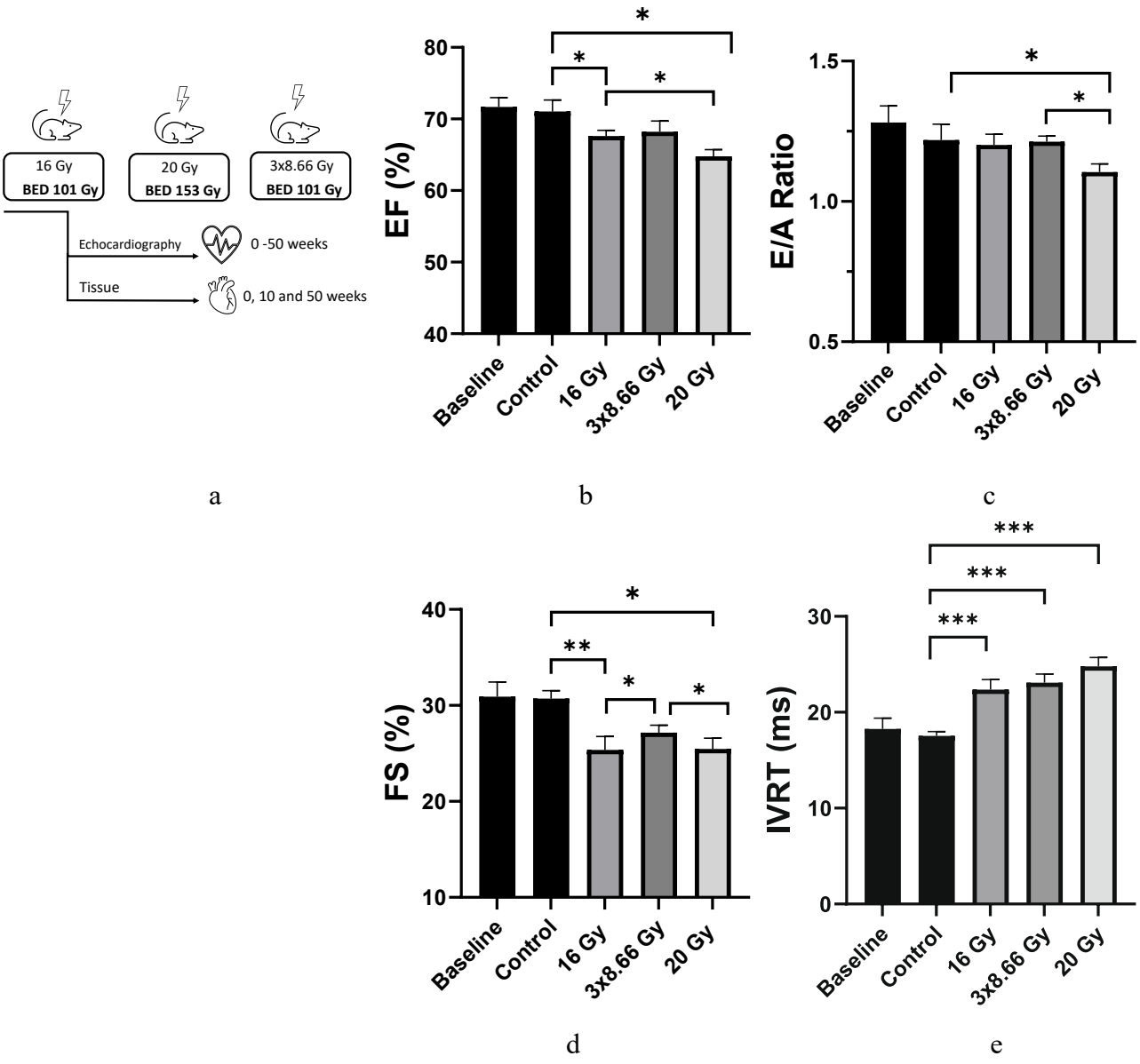

Fig. 1. Schematic representation of the experimental design and calculated biological effective doses for the different treatment protocols (a) and differences in systolic (b, d) and diastolic (c, e) function at 50 weeks after cardiac base irradiation. Data are presented as an average of 7 mice per treatment group ± standard error of the mean, against the baseline and age-matched control values (n = 3). Significance values were classified as *P < 0.05, **P < 0.01 and ***P < 0.001.

remained within tolerated weight loss of < 15 %. All experimental procedures were conducted in accordance with the Home Office Guidance on the Operation of the Animals (Scientific Procedures) Act 1986, published by Her Majesty's Stationary Office, London, and approved by the institutional Animal Welfare and Ethical Review Body (PPL2813). Animal studies are reported in compliance with the ARRIVE guidelines [15,16] and suggested reporting requirements for preclinical cardiac irradiation studies [8].

Imaging, treatment planning and irradiation

Mice were irradiated with 220 kVp X-rays under CBCT image guidance using a Small Animal Radiation Research Platform (SARRP, Xstrahl Life Sciences) calibrated using the Institute of Physics and Engineering in Medicine and Biology (IPEMB) code of practice [17]. Fig. 1a shows a diagram of the study design, including the calculated biological effective doses (BED). Mice were randomized prior to irradiation in treatment groups of a single dose of 16 Gy or 20 Gy or with 3 fractions of 8.66 Gy on consecutive days, and CBCT only. For irradiations, animals were anaesthetised with ketamine and xylazine (100 mg/kg and 10 mg/kg) by intraperitoneal injection. The base of the heart was irradiated using parallel opposed fields delivered using a 3 x 9 mm collimator (dose rate 2.67 ± 0.11 Gy/min with a 0.5 mm Cu filter) as previously described [10]. Control animals were anaesthetised and CBCT imaged using the SARRP.

Doses were selected based on previous work [9], and BED values were 101.3 Gy, 153.3 Gy and 101.3 Gy for 16 Gy, 20 Gy and 3 x 8.6 Gy, respectively. BED was calculated using:

$$BED = \frac{E}{\alpha} = (nd)\left(1 + \frac{d}{\frac{\alpha}{\beta}}\right) \quad (1)$$

where n is the number of fractions, d is the dose per fraction and using an α/β ratio of 3 Gy for the heart [18].

CBCT scans were performed for treatment planning and dose volume histograms (DVHs) were extracted from Muriplan (Xstrahl, Suwannee, GA), see Supplementary Fig. 1a)-d) with a representative DVH showing the dose to the left and right lung. Mean heart dose (MHD) and the heart volume receiving at least 5 Gy (V5) were extracted from the individual DVHs using Matlab (R2022a) and shown in Supplementary Fig. 1 d) and e).

Echocardiography

Longitudinal transthoracic echocardiography (TTE) was performed at baseline and at 10-week intervals up to 50 weeks after irradiation using a Vevo3100® ultrasound system using the MX550D scan head (Fujifilm VisualSonics Inc. ON, Canada), and data were extracted as previously described [9]. During TTE acquisition, animals were anaesthetised using 2 % isoflurane. Parasternal long axis videos were used for GLS and segmental longitudinal strain analysis using Vevo Strain package (Fujifilm VisualSonics Inc.) after the endocardium was semi-automatically traced, and three consecutive cardiac cycles were selected [14,19]. For segmental strain, the values presented are an average between the anterior and posterior peak strain values for basal and apical segments. Post-processed strain data along with left ventricle end-systolic mass (ESLVM) and end diastolic mass (EDLVM), end systole volume (ESV) and end diastole volume (EDV) were exported and analysed using GraphPad Prism9 (Version 9.0, GraphPad Software, Inc.). Observers were blinded to the experimental groups during data acquisition and analysis.

Histological assessment of cardiac fibrosis

Mice were culled by cervical dislocation at baseline and 50 weeks after irradiation. Hearts were removed and mid-line dissected in the transverse plane and placed into cassettes to ensure correct orientation of the tissue before being fixed in 10 % formalin for 24 h at room temperature. After fixation, hearts were paraffin embedded and processed for histological evaluation. Staining was performed using Mayer's haematoxylin and eosin (90 % ethanol-based) stain or picrosirius red stain (Abcam, ab150681). Slides were viewed by bright-field microscopy (Olympus CKX41, DP25 camera) and analysed using the open-source platform ImageJ [20]. Fibrosis was analysed as the myocardial collagen (MC) deposition using a manual threshold contouring for Red-Green-Blue (RGB) texture analysis. For each sample, the percentage of myocardial collagen was calculated as the average percentage of picrosirius red staining relative to the total tissue in five different fields of view within the cranial third or the apex of the heart.

Data and statistical analysis

Statistical differences between populations were calculated using unpaired two-tailed Student t-tests, or one way ANOVA tests where appropriate, with a significance threshold of 0.05. Data are presented either as the average for the entire experimental arm ± standard error, or per individual mouse in box and whisker plots showing the lower (Q1), upper (Q3) quartiles and the median value. Prism (Version 9.0, GraphPad Software, Inc.) was used for all plots and statistical calculations. Statistical significance has been tested for both baseline and age matched control values. No significant difference was found between baseline values and age-matched control values. For simplicity, the discussed differences are presented compared to age matched controls.

Correlation between functional parameters and MC was tested by fitting linear regression lines using Prism with the R^2 values reported. Statistical significance of slope parameters was calculated using an F-test comparing the linear regression model to a model with a slope of 0.

Results

Longitudinal assessment of cardiac function showed the most significant changes at 50 weeks after irradiation as shown in Fig. 1(b-e). Systolic function measured by ejection fraction (EF) was significantly decreased in all groups compared to baseline and age-matched control animals ($p = 0.03$) with the largest decrease observed following 20 Gy irradiation (control = 71.06 ± 1.9 %, 20 Gy = 64.79 ± 4.3 %) ($p = 0.031$). 16 Gy and 3 x 8.66 Gy irradiations resulted in similar small but significant decrease in EF compared to age-matched controls (16 Gy = 64.79 ± 4.3 %, 3 x 8.6 Gy = 67.62 ± 3.5 %) ($p = 0.027$). Similarly, fractional shortening (FS) was significantly decreased in all groups compared to baseline and age-matched controls ($p < 0.007$) with the largest decreases observed following treatment with 16 Gy and 20 Gy (control = 30.72 ± 3.6 %, 16 Gy = 25.38 ± 3.18 %, 3 x 8.6 Gy = 27.58 ± 2.36 %, 20 Gy = 25.45 ± 2.15 %) ($p < 0.007$).

Diastolic function measured by the E/A ratio was decreased in all groups with the most significant changes observed following treatment with 20 Gy (control = 1.21 ± 0.11, 20 Gy = 1.10 ± 0.03). Treatment with 16 Gy or 3 x 8.66 Gy resulted in similar decreases in E/A ratio (16 Gy = 1.20 ± 3.6 %, 3 x 8.6 Gy = 1.21 ± 2.8 %). The isovolumic relaxation time (IVRT) between aortic valve closure and mitral valve opening was significantly increased in all groups compared to baseline and age-matched controls with the most significant increase observed following treatment with 20 Gy (control = 17.54 ± 1.16 ms, 16 Gy = 22.36 ± 2.01 ms, 3 x 8.6 Gy = 23.09 ± 3.5 ms, 20 Gy = 24.78 ± 1.28 ms). The overall changes in the systolic and diastolic parameters showed a BED-dependent relationship that was inversely related to EF, FS and E/A and positively related to IVRT. No significant changes in systolic and diastolic parameters were observed at 10 weeks after irradiation (Supplementary Fig. 2). Longitudinal measurements at 10-week intervals for irradiated animals are presented in Supplementary Fig. 3. No significant differences were observed between the baseline systolic and diastolic

parameters and the age-matched control animals. Data for control animals at each time point showed no significant age dependence and are shown in Supplementary Fig. 4.

Cardiac strain uses two-dimensional speckle tracking TTE (2D-STE) to assess global and regional deformation of the myocardium during the cardiac cycle [21]. At 10 weeks, GLS was significantly decreased in each of the treatment groups with a strong BED-dependence (Fig. 2a). Myocardial performance index (MPI) is a combined measure of systolic and diastolic performance that was not significantly changed at 10 weeks (Fig. 2c). At 50 weeks, the overall trends in GLS were similar to those observed at 10 weeks with all irradiated groups showing reductions in GLS. Unirradiated control animals showed no significant changes in GLS compared to 10 weeks ($p > 0.05$) Supplementary Fig. 4. MPI was significantly increased in all irradiated animals at 50 weeks indicating detectable changes in cardiac function. These data suggest that GLS may be an imaging biomarker of early radiation-induced cardiac dysfunction that is not detectable based on TTE measures of systolic and diastolic function.

Segmental analysis was used to compare changes in segmental LS (SLS) in the base and apex of the heart (Fig. 3). For the age-matched controls, no significant differences were observed in SLS across all animals (Fig. 3a, $p > 0.05$). At 10 weeks, segmental LS in the base and apex of the heart followed a similar BED dependent trend overall, with SLS levels significantly lower in the base segment (Fig. 3b). At 50 weeks post-irradiation, SLS in the base was not significantly lower for the various treatment groups compared to those observed at 10 weeks ($p > 0.05$). In contrast, significant decreases in apical SLS were observed for all irradiated groups at 50 weeks compared to 10 weeks ($p < 0.01$). These data demonstrate SLS changes 50 weeks after irradiation of the heart base, with apical strain delay at 10 weeks but resolved to a level comparable to the base strain at 50 weeks.

Cardiac remodelling describes a range of molecular, cellular, and interstitial changes manifested as changes in size, mass, geometry, and function of the heart after injury [22]. Changes in the geometry, mass, and volume of the LV were assessed at 10 and 50 weeks after irradiation. At 50 weeks, significant increases in all LV systolic and diastolic

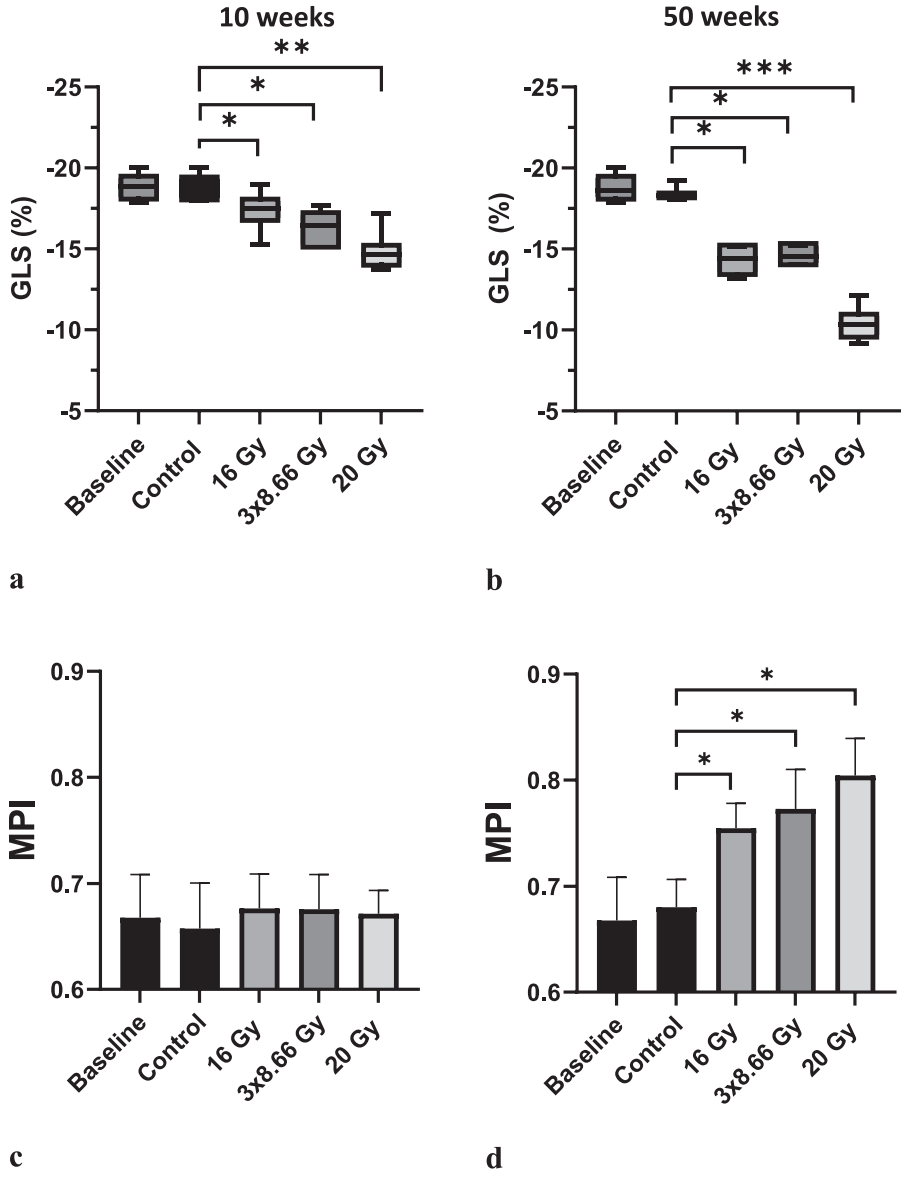

Fig. 2. Variations in global longitudinal strain (GLS) and myocardial performance index (MPI) at 10 (a, c) and 50 weeks (b, d) after cardiac base irradiation. GLS data are presented as box-and-whiskers plot showing the lower (Q1), upper (Q3) quartiles and the median value. GLS is compared to baseline ($n > 7$) and age-matched control ($n = 3$) measurements. MPI data are presented as an average of 7 mice per treatment group ± standard error of the mean and compared to the baseline levels before irradiation and age-matched controls ($n = 3$). Significance values were classified as *$P < 0.05$, **$P < 0.01$ and ***$P < 0.001$.

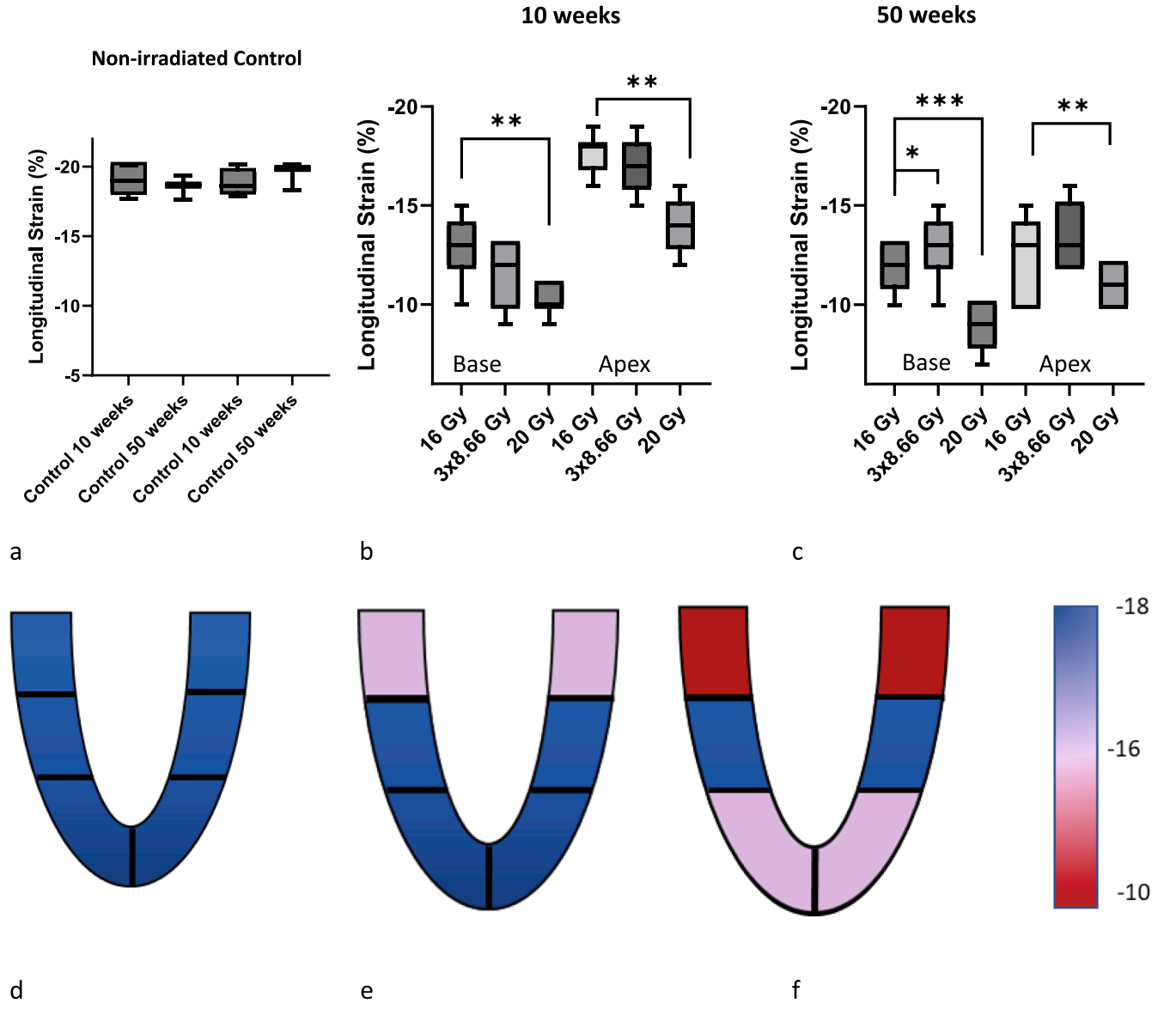

Fig. 3. Longitudinal variations in segmental strain represented as the segmental longitudinal strain (SLS) in the base and apex of the heart. Data are shown for age-matched control values (n = 3) (a) and at 10 (b) and 50 weeks (c) after cardiac base irradiation. Data are presented for 7 mice per treatment group as box-and-whiskers plot showing the lower (Q1) and upper (Q3) quartiles and the median. Corresponding schematics are presented in (d), (e) and (f). Significance values were classified as *P < 0.05, **P < 0.01 and ***P < 0.001.

remodelling parameters were observed compared to age-matched controls and baseline levels (Fig. 4, $p < 0.05$). In contrast to the observed changes in systolic, diastolic function and GLS, changes in cardiac remodelling parameters were not significantly different across all the irradiation schedules in the study ($p > 0.05$). Similar trends were observed at 10 weeks after irradiation with the overall values lower than those observed at 50 weeks (Supplementary Fig. 3). Myocardial fibrosis at 50 weeks was significantly increased in the base and apex of the heart in all irradiated groups compared to baseline and age-matched controls (Fig. 4e, $p < 0.05$). The levels of myocardial collagen (MC) observed in the base and apical regions were not directly related to the BED. Representative images from picrosirius red staining for myocardial collagen are shown in Supplementary Figure 6.

The levels of myocardial fibrosis in the base of the heart were differentially correlated to cardiac function and GLS at 50 weeks after irradiation (Fig. 5). FS showed a significant linear correlation ($R^2 = 0.49$) with the levels of MC ($p < 0.01$) across each of the treatment groups, indicating an inverse relationship between these parameters (Fig. 5c). In contrast, EF ($R^2 = 0.07$) and MPI ($R^2 = 0.07$) were not significantly correlated with the levels of MC across each of the treatment groups (Fig. 5a & b, $p > 0.05$). Additionally, GLS was significantly correlated with MC ($R^2 = 0.22$, $p = 0.02$) indicating a positive relationship between these parameters (Fig. 5d).

Discussion

Heart dose has emerged as an independent predictor of overall survival in patients with NSCLC treated with radiotherapy [23]. Several studies have identified the base of the heart as a region of enhanced dose sensitivity and a potential target for cardiac sparing. In agreement with clinical observations, the base of the heart has previously been described as a differentially radiosensitive sub-volume that results in changes in cardiac structure, function, and gene expression [9,10]. In this study, we applied a late RICT heart base model to assess dose-dependent functional changes following single and fractionated treatments and to analyse the deformation and remodelling following base irradiation.

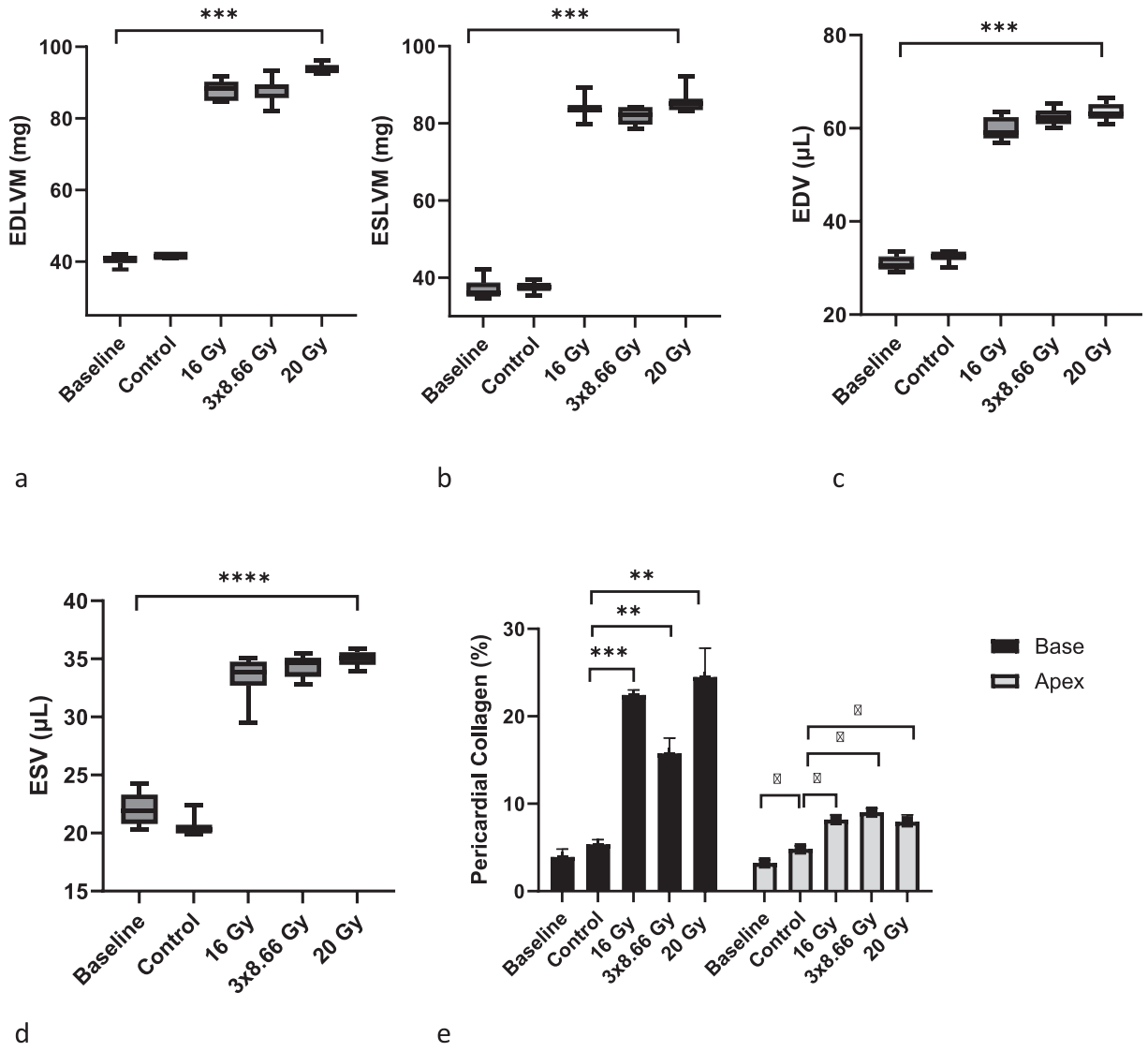

Fig. 4. Variations in left ventricular (LV) cardiac remodelling and fibrosis at 50 weeks after cardiac base irradiation for a) End diastolic LV mass (EDLVM), b) end systolic LV mass (ESLVM), c) End Diastolic Volume (EDV) and d) End Systolic Volume (ESV). Data are presented as box-and-whiskers plot showing the lower (Q1) and upper (Q3) quartiles and the median against baseline ($n > 7$) and age-matched controls ($n = 3$). e) myocardial collagen level in the base (black columns) and apex of the heart (grey columns). Histology data are presented as an average of 6 mice per treatment group for baseline and 2 age-matched controls ± standard error of the mean. Significance values were classified as $^*p < 0.05$, $^{**}p < 0.01$ and $^{***}p < 0.001$.

In agreement with previous reports, we showed that irradiation of the heart base leads to significant loss of systolic and diastolic function measured by TTE [9,10]. Furthermore, we showed that the systolic and diastolic parameters are dependent on BED: inversely related to EF, FS and E/A yet positively related to IVRT. Despite the advantages of TTE, the manifestation of late occurring radiation-induced changes in cardiac function has variable latency after treatment [11]. TTE also is limited by variations in the quality of images during acquisition, off axis artefacts and the movement of the thorax during the respiratory and cardiac cycles.

We report early changes in global and segmental LS using 2D-STE in response to RT. This approach uses acoustic markers and their relative motion to detect subtle changes in myocardial contractility and deformation rate that are specific metrics of subclinical disease [24]. Whilst this approach remains reliant on high quality images, it is a more reliable approach as it directly measures myocardial deformation compared to other TTE parameters based on the measurement of calculated cardiac volumes. The application of TTE to assess changes in cardiac strain after RT is an emerging area having been previously used in a preclinical rat model [13]. However, cardiac strain can also be quantified using MRI-generated strain parameters. This approach has been used to assess the spatial and temporal progression of regional cardiac dysfunction post-RT following whole heart or whole-body irradiation in rats [25–27].

In our model, we show that GLS can accurately detect BED-dependent radiation-induced changes in cardiac strain at 10 weeks after treatment. Importantly, the observed decreases in GLS at 10 weeks were indicative of variations at 50 weeks. Similar differences were observed in the heart base at 10 and 50 weeks after treatment using SLS analysis. In contrast, apical SLS at 10 weeks was significantly higher compared to basal SLS which was not predictive of the observed SLS levels at 50 weeks. Collectively, these data clearly demonstrate the potential use of GLS as an imaging biomarker of early radiation-induced cardiac dysfunction before detectable systolic and diastolic dysfunction. Furthermore, segmental LS can be used to resolve regional variations in strain following targeted irradiation of cardiac sub-volumes.

Cardiac remodelling is a complex pathological response involving multiple processes including a range of molecular, cellular, and

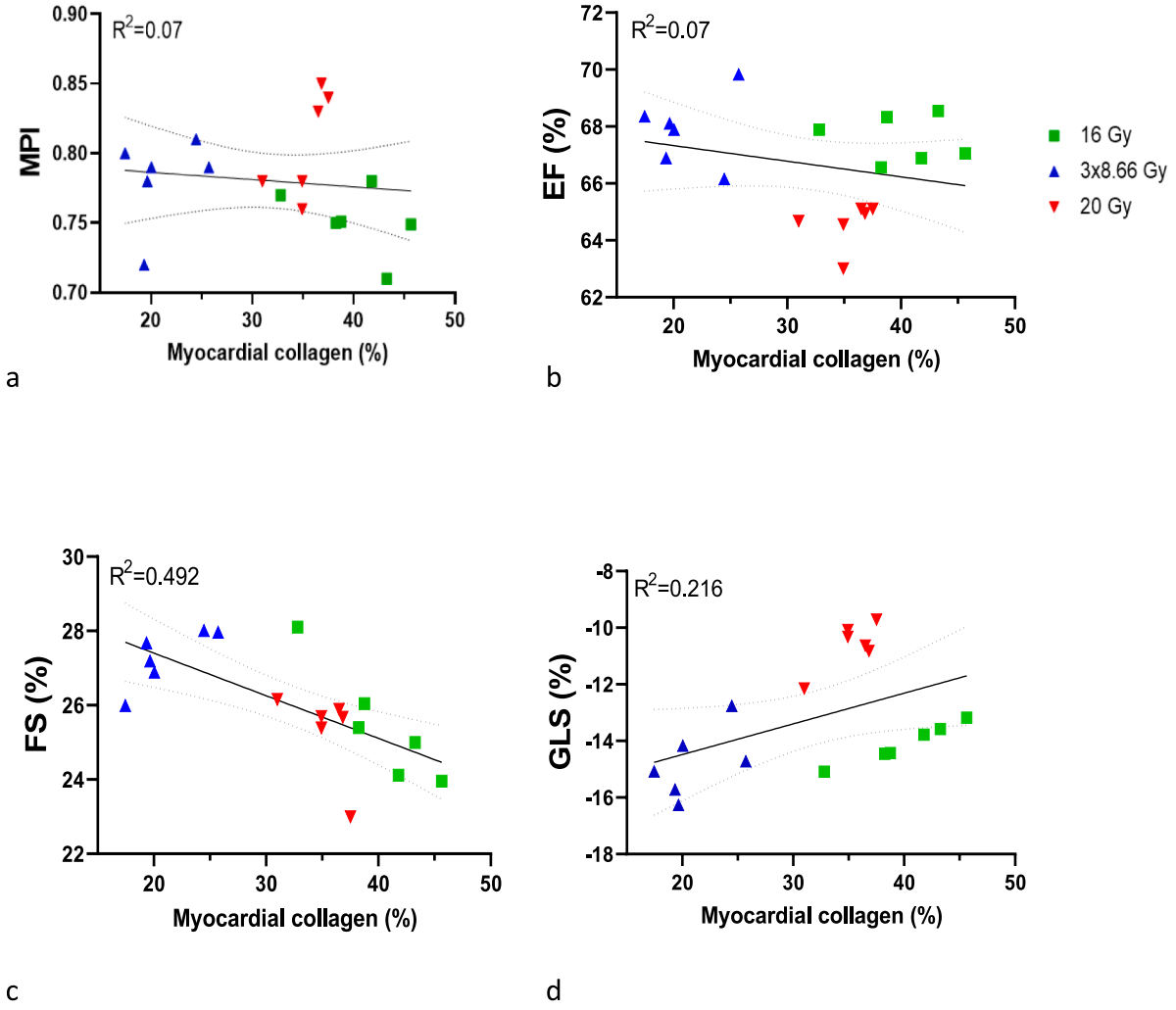

Fig. 5. Correlations between myocardial collagen in the heart base with a) myocardial performance index (MPI), b) ejection fraction (EF), c) fractional shortening (FS) and global longitudinal strain (GLS) at 50 weeks after cardiac base irradiation. Data are presented for 6 in dividual mice from each treatment group.

interstitial changes, manifested as changes in size, mass, geometry, and function of the heart after injury [22,28]. Clinically, thoracic irradiation has been shown to increase the risk of cardiac remodelling in adult survivors of childhood cancer [28] yet the impact of cardiac dose distributions on remodelling is not well established. In this study, base irradiation significantly increased end systolic and end diastolic mass and volume yet the observed changes were independent of BED.

Collagen deposition and fibrosis are a well-established sequalae of incidental radiation exposure on many organs including the heart [29]. Myocardial collagen (MC) increases the stiffness of the myocardium leading to the development of fibrosis; a process characterized by decreased ventricular elasticity and distensibility that can result in cardiac dysfunction [29,30]. In agreement with these previous studies, MC levels in the heart base were not related to BED whilst MC in the apex was lower compared to the base and showed a clear BED-dependence. The levels of MC in the base were not correlated with MPI or EF but were inversely correlated with FS ($R^2 = 0.49$) and directly correlated with GLS ($R^2 = 0.22$). These changes reflect complex regional interactions in the response to radiation in cardiac deformation and contractility that result in both systolic and diastolic dysfunction 50 weeks after irradiation.

This study provides a detailed evaluation of BED-dependent changes in the heart following base irradiation and for the first-time reports on GLS changes following sub-volume irradiation. We hypothesise the observed effects are related to the complexity of the heart base including vascular structures (the aorta, superior vena cava and proximal coronary arteries) and conduction tissue including the sinoatrial and atrioventricular nodes. Using spatial transcriptomics, we previously reported that base irradiation results in differential gene expression affecting the upregulation of immune-related processes and the downregulation of calcium transmembrane transporter activity, regulation of heart contraction and cytokine-mediated pathways [10]. At the mechanistic level, we hypothesize that these processes are similarly involved at different BEDs yet further studies are required across a wider range of doses and fractionation schedules. The limited fractionated data presented in this study clearly demonstrate the targeting accuracy and reproducibility of our experimental setup. Also, our radiobiological modelling assumed an α/β ratio of 3 Gy based on whole heart exposures which is also accurate for partial heart exposures observed in this study. Furthermore, the similar BED between the single fraction and fractionated schedules highlights the importance of BED on the fractionation schedules involved in preclinical RICT models. Several studies using prolonged fractionation schedules mirroring clinical exposures report no functional effects in preclinical models [13,31].

It is important to acknowledge that our model does not accurately recapitulate clinical dose distributions in patients receiving RT for lung cancer that includes a significant dose bath to the lungs that may impact on cardiac response [32]. Also, whilst mouse models have utility in

cardiovascular research, they do not fully recapitulate all the characteristics of the human disease phenotype [7], which may limit interpretation of our experimental data. Another limitation of the study consists in the group size for the age-matched control animals. Further correlation with biomarkers of RICT needs to also be explored in this preclinical system, as this model may provide insight into dose dependency of various substructures.

In conclusion, we have characterised dose-dependent changes in cardiac function, deformation and remodelling in a preclinical model of heart base irradiation. We report on the use of GLS as an early imaging biomarker of late occurring cardiac dysfunction that can also be used to resolve segmental strain following base irradiation.

CRediT authorship contribution statement

Mihaela Ghita-Pettigrew: Writing – review & editing, Writing – original draft, Methodology, Investigation, Formal analysis, Data curation. **Kevin S. Edgar:** Writing – original draft, Investigation, Formal analysis. **Refik Kuburas:** Writing – original draft, Investigation, Data curation. **Kathryn H. Brown:** Writing – review & editing, Writing – original draft, Investigation, Formal analysis, Data curation. **Gerard M. Walls:** Writing – review & editing, Writing – original draft, Project administration, Data curation, Conceptualization. **Cecilia Facchi:** Writing – review & editing, Writing – original draft, Visualization, Investigation, Data curation. **David J. Grieve:** Writing – original draft, Supervision, Resources, Methodology, Conceptualization. **Chris J. Watson:** Writing – original draft, Methodology, Funding acquisition, Conceptualization. **Alan McWilliam:** Writing – original draft, Validation, Methodology, Conceptualization. **Marcel van Herk:** Writing – original draft, Validation, Methodology. **Kaye J. Williams:** Writing – original draft, Validation, Methodology, Conceptualization. **Karl T. Butterworth:** Writing – review & editing, Writing – original draft, Supervision, Project administration, Methodology, Investigation, Funding acquisition, Data curation, Conceptualization.

Declaration of competing interest

The authors declare that they have no known competing financial interests or personal relationships that could have appeared to influence the work reported in this paper.

Acknowledgements

This work was funded by the Medical Research Council [MR/V009605/1]. GW is supported by a Cancer Research UK Post-doctoral Bursary Award (RCCPOB-Nov22/100010). KSE and DJG are supported by the British Heart Foundation (PG/15/18/31333).

Appendix A. Supplementary material

Supplementary data to this article can be found online at https://doi.org/10.1016/j.radonc.2024.110113.

References

[1] Hu X, He W, Wen S, Feng X, Fu X, Liu Y, et al. Is IMRT superior or inferior to 3DCRT in radiotherapy for NSCLC? A meta-analysis. PLoS One 2016;11. https://doi.org/10.1371/journal.pone.0151988.
[2] Atkins KM, Rawal B, Chaunzwa TL, Lamba N, Bitterman DS, Williams CL, et al. Cardiac radiation dose, cardiac disease, and mortality in patients with lung cancer. J Am Coll Cardiol 2019;73:2976–87. https://doi.org/10.1016/j.jacc.2019.03.500.
[3] Banfill K, Giuliani M, Aznar M, Franks K, McWilliam A, Schmitt M, et al. Cardiac toxicity of thoracic radiotherapy: Existing evidence and future directions. J Thorac Oncol 2021;16:216–27. https://doi.org/10.1016/j.jtho.2020.11.002.
[4] Bergom C, Bradley JA, Ng AK, Samson P, Robinson C, Lopez-Mattei J, et al. Past, present, and future of radiation-induced cardiotoxicity: Refinements in targeting, surveillance, and risk stratification. JACC CardioOncol 2021;3:343–59. https://doi.org/10.1016/j.jaccao.2021.06.007.
[5] McWilliam A, Kennedy J, Hodgson C, Vasquez Osorio E, Faivre-Finn C, van Herk M. Radiation dose to heart base linked with poorer survival in lung cancer patients. Eur J Cancer 2017;85:106–13. https://doi.org/10.1016/j.ejca.2017.07.053.
[6] Craddock M, Nestle U, Koenig J, Schimek-Jasch T, Kremp S, Lenz S, et al. Cardiac function modifies the impact of heart base dose on survival: A voxel-wise analysis of patients with lung cancer from the PET-plan trial. J Thorac Oncol 2023;18:57–66. https://doi.org/10.1016/j.jtho.2022.09.004.
[7] Milani-Nejad N, Janssen PML. Small and large animal models in cardiac contraction research: Advantages and disadvantages. Pharmacol Ther 2014;141:235–49. https://doi.org/10.1016/j.pharmthera.2013.10.007.
[8] Walls GM, O'Kane R, Ghita M, Kuburas R, McGarry CK, Cole AJ, et al. Murine models of radiation cardiotoxicity: A systematic review and recommendations for future studies. Radiother Oncol 2022;173:19–31. https://doi.org/10.1016/j.radonc.2022.04.030.
[9] Ghita M, Gill EK, Walls GM, Edgar KS, McMahon SJ, Osorio EV, et al. Cardiac subvolume targeting demonstrates regional radiosensitivity in the mouse heart. Radiother Oncol 2020;152:216–21. https://doi.org/10.1016/j.radonc.2020.07.016.
[10] Walls GM, Ghita M, Queen R, Edgar KS, Gill EK, Kuburas R, et al. Spatial gene expression changes in the mouse heart after base-targeted irradiation. Int J Radiat Oncol Biol Phys 2023;115:453–63. https://doi.org/10.1016/j.ijrobp.2022.08.031.
[11] Patel J, Rikhi R, Hussain M, Ayoub C, Klein A, Collier P, et al. Global longitudinal strain is a better metric than left ventricular ejection fraction: Lessons learned from cancer therapeutic-related cardiac dysfunction. Curr Opin Cardiol 2020;35:170–7. https://doi.org/10.1097/HCO.0000000000000716.
[12] Walker V, Lairez O, Fondard O, Jimenez G, Camilleri J, Panh L, et al. Myocardial deformation after radiotherapy: A layer-specific and territorial longitudinal strain analysis in a cohort of left-sided breast cancer patients (BACCARAT study). Radiat Oncol 2020;15. https://doi.org/10.1186/s13014-020-01635-y.
[13] Ribeiro S, Simões AR, Rocha F, Vala IS, Pinto AT, Ministro A, et al. Molecular changes in cardiac tissue as a new marker to predict cardiac dysfunction induced by radiotherapy. Front Oncol 2022;12. https://doi.org/10.3389/fonc.2022.945521.
[14] Domenica Rea, Carmela Coppola, Antonio Barbieri, Maria Gaia Monti, Gabriella Misso, Giuseppe Palma, et al. Strain Analysis in the Assessment of a Mouse Model of Cardiotoxicity due to Chemotherapy: Sample for Preclinical Research. In Vivo (Brooklyn) 2016:279–90.
[15] Kilkenny C, Browne WJ, Cuthill IC, Emerson M, Altman DG. The ARRIVE guidelines checklist animal research : Reporting in vivo experiments. Br J Pharmacol 2010;8:8–9. https://doi.org/10.1371/journal.pbio.1000412.
[16] du Sert NP, Ahluwalia A, Alam S, Avey MT, Baker M, Browne WJ, et al. Reporting animal research: Explanation and elaboration for the arrive guidelines 2.0. PLoS Biol 2020;18. https://doi.org/10.1371/journal.pbio.3000411.
[17] Rosser KE. The IPEMB code of practice for the determination of absorbed dose for x-rays below 300 kV generating potential (0.035 mm Al-4 mm Cu HVL; 10–300 kV generating potential). Inst Phys Eng Med Biol Phys Med Biol 1996;41:2605–25. https://doi.org/10.1088/0031-9155/50/12/001.
[18] Boerma M, Sridharan V, Mao XW, Nelson GA, Cheema AK, Koturbash I, et al. Effects of ionizing radiation on the heart. Mutat Res Rev Mutat Res 2016;770:319–27. https://doi.org/10.1016/j.mrrev.2016.07.003.
[19] Bauer M, Cheng S, Unno K, Lin FC, Liao R. Regional cardiac dysfunction and dyssynchrony in a murine model of afterload stress. PLoS One 2013;8. https://doi.org/10.1371/journal.pone.0059915.
[20] Schneider CA, Rasband WS, Eliceiri KW. NIH Image to ImageJ: 25 years of Image Analysis HHS Public Access. vol. 9. 2012.
[21] Koshizuka R, Ishizu T, Kameda Y, Kawamura R, Seo Y, Aonuma K. Longitudinal strain impairment as a marker of the progression of heart failure with preserved ejection fraction in a rat model. J Am Soc Echocardiogr 2013;26:316–23. https://doi.org/10.1016/j.echo.2012.11.015.
[22] Cohn JN, Ferrari R, Sharpe N. Cardiac Remodeling-Concepts and Clinical Implications: A Consensus Paper From an International Forum on Cardiac Remodeling. 2000.
[23] Bradley JD, Paulus R, Komaki R, Masters G, Blumenschein G, Schild S, et al. Standard-dose versus high-dose conformal radiotherapy with concurrent and consolidation carboplatin plus paclitaxel with or without cetuximab for patients with stage IIIA or IIIB non-small-cell lung cancer (RTOG 0617): a randomised , two-by-two factoria n.d.:187–99. https://doi.org/10.1016/S1470-2045(14)71207-0.
[24] Mor-Avi V, Lang RM, Badano LP, Belohlavek M, Cardim NM, Derumeaux G, et al. Current and evolving echocardiographic techniques for the quantitative evaluation of cardiac mechanics: ASE/EAE consensus statement on methodology and indications: Endorsed by the Japanese Society of Echocardiography. J Am Soc Echocardiogr 2011;24:277–313. https://doi.org/10.1016/j.echo.2011.01.015.
[25] Baker JE, Fish BL, Su J, Haworth ST, Strande JL, Komorowski RA, et al. 10 Gy total body irradiation increases risk of coronary sclerosis, degeneration of heart structure and function in a rat model. Int J Radiat Biol 2009;85:1089–100. https://doi.org/10.3109/09553000903264473.
[26] Ibrahim ESH, Baruah D, Budde M, Rubenstein J, Frei A, Schlaak R, et al. Optimized cardiac functional MRI of small-animal models of cancer radiation therapy. Magn Reson Imaging 2020;73:130–7. https://doi.org/10.1016/j.mri.2020.08.020.
[27] Ibrahim ESH, Sosa A, Brown SA, An D, Klawikowski S, Baker J, et al. Myocardial contractility pattern characterization in radiation-induced cardiotoxicity using magnetic resonance imaging: A pilot study with ContractiX. Tomography 2023;9:36–49. https://doi.org/10.3390/tomography9010004.
[28] Jefferies JL, Mazur WM, Howell CR, Plana JC, Ness KK, Li Z, et al. Cardiac remodeling after anthracycline and radiotherapy exposure in adult survivors of

childhood cancer: A report from the St Jude Lifetime Cohort Study. Cancer 2021; 127:4646–55. https://doi.org/10.1002/cncr.33860.
[29] Dreyfuss AD, Velalopoulou A, Avgousti H, Bell BI, Verginadis II. Preclinical models of radiation-induced cardiac toxicity: Potential mechanisms and biomarkers. Front Oncol 2022;12. https://doi.org/10.3389/fonc.2022.920867.
[30] Wang B, Wang H, Zhang M, Ji R, Wei J, Xin Y, et al. Radiation-induced myocardial fibrosis: Mechanisms underlying its pathogenesis and therapeutic strategies. J Cell Mol Med 2020;24:7717–29. https://doi.org/10.1111/jcmm.15479.
[31] Lee CL, Lee JW, Daniel AR, Holbrook M, Hasapis S, Wright AO, et al. Characterization of cardiovascular injury in mice following partial-heart irradiation with clinically relevant dose and fractionation. Radiother Oncol 2021; 157:155–62. https://doi.org/10.1016/j.radonc.2021.01.023.
[32] Van Luijk P, Novakova-Jiresova A, Faber H, Schippers JM, Kampinga HH, Meertens H, et al. Radiation Damage to the Heart Enhances Early Radiation-Induced Lung Function Loss. n.d.